OPTICAL ABSORPTION AND EMISSION FROM

M-CENTERS IN MgF$_2$

By

LEONARD NORMAN FEUERHELM, JR.

Bachelor of Science

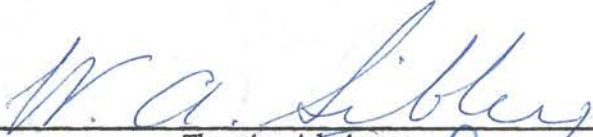Oklahoma State University

Stillwater, Oklahoma

1970

Submitted to the Faculty of the Graduate College
of the Oklahoma State University
in partial fulfillment of the requirements
for the Degree of
MASTER OF SCIENCE
July, 1973

OPTICAL ABSORPTION AND EMISSION FROM
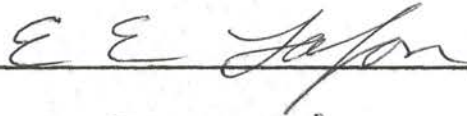
M—CENTERS IN MgF_2
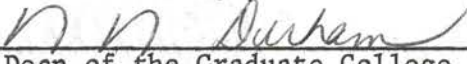
Thesis Approved:

_____
Thesis Adviser

_____

_____
E E Lason

_____
Dean of the Graduate College

ACKNOWLEDGEMENTS

TABLE OF CONTENTS

LIST OF FIGURES

CHAPTER I

INTRODUCTION

In the study of solid state physics, the defect solid state is
vitally important. The study of imperfection in solids increases our
knowledge and understanding of the perfect lattice and also leads to the
development of many technological devices. Several recent advances have
come about because of such studies, and the future indicates more are to
come. Solid state lasers are constructed from crystals containing de-
fects, and much of the technology of the current electronics industry
owes its existence to imperfections in solids. In the not too distant
future there is the promise of high density information storage unit for
computers, and totally new means of information display, both temporary
and permanent.

There are many methods of investigating defects in solids, among
them mechanical, optical, electrical, and thermal techniques (1). Of
these, optical studies yield the greatest amount of information although
these techniques are not applicable to every crystal. Insulating crys-
tals, and especially polar insulators, are especially well suited to
this experimental technique as they are often transparent over wide
ranges of wavelength.

There are two main categories of defects: point defects and line
defects (2). The extended type defects include dislocations, grain
boundaries, and macroscopic inclusions. The point defects include single

1

or small groups of ions missing from lattice sites called vacancies, ions in non-lattice sites known as interstitials, and impurity ions which have gone in substitutionally for lattice ions and are called impurities. In this study, we are concerned with lattice vacancies containing trapped electrons, either singly or in very small groups. This type of point defect is often called a color center, because, as early workers in the field noticed, their presence often introduces visible coloration into a normally transparent host crystal. It is this coloration which makes it feasible to study these crystals optically, because much information can be obtained from the absorption energy and shape of the absorption band.

Defects may be introduced into a crystal by several means, including mechanical deformation (3), additive coloration (4,5), and irradiation (6). Mechanical deformation, created by bending, squeezing, or indenting the crystal, tends to create extended defects so it is seldom used when one is studying point defects. Additive coloration is accomplished by heating the host crystal in the vapor of one of its constituent elements—usually the cation or positive ion. As ions in the vapor and in the crystal come into equilibrium, simple anion vacancies are introduced into the crystal lattice. This technique introduces only the simplest of defects, but it is often used for just this very reason. Irradiation is the most common of the defect forming techniques. With this method crystals are bombarded with energetic particles, such as electrons, neutrons, or photons (gamma rays), producing damage within the lattice. Even though the damage produces many types of defects, there is seldom much trouble in isolating and studying only one particular kind, as the defects tend to be widely scattered and therefore do

not interact with each other. Another reason for using the irradiation technique is that some defects are not producable by any other technique, so that irradiation is required in order to study these types of defects.

Of these three types mentioned, only irradiation was employed in this study. The damage was induced by electrons accelerated by a Van de Graaff accelerator. The major defects that such irradiation produces are an interstitial ion and an anion vacancy which is occupied by an appropriate number of electrons so as to retain electrical neutrality with the crystal. This latter defect is called the F center (6). Aggregates of F-centers are also well known, and are formed when two or more F-type centers are in adjacent anion sites in the crystal lattice. This study is concerned with an F-aggregate center in magnesium fluoride (MgF_2). The center is called the M center, and will be fully described in the next chapter.

In this study, we examine MgF_2 by optical means, and investigate in detail the changes with temperature of the peak position and the full width at half maximum of the absorption and luminescence bands due to the center so that some idea of the interaction of lattice modes with defects can be obtained.

CHAPTER II

THEORY

M-Center Symmetry Considerations in MgF_2

A model for the center responsible for the M band absorption was
first given by Seitz (7). The model consisted of an F-center, and anion
vacancy containing a single electron for charge neutrality, associated
with a neutral vacancy pair. Van Doorn and Haven (8) later showed that
a pair of adjacent F-centers is the correct model (9). In the rutile
structure of MgF_2, there are four possible types of M centers, as shown
in Figure 1. Each type has a distinctive symmetry and should exhibit
different optical properties.

Since the symmetry of each type is important, a discussion of these
will be useful. The first type lies along the c-axis, with the unique
C_2 axis along either the [110] or [1$\bar{1}$0] direction, depending on its lo-
cation within the unit cell. The symmetry, then, is C_{2v}, and the defect
can be easily identified by the label C_{2v} in the figure. We shall refer
to it as the $M(C_{2v})$ center.

A second type of M center consists of adjacent anion sites lying in
the top plane of the unit cell along the [110] or [1$\bar{1}$0] directions.
These defects, labelled by D_{2h} in the figure, have orthorhombic D_{2h}
symmetry. The three C_2 axes for this defect lie along [110], [1$\bar{1}$0], and
[001] directions.
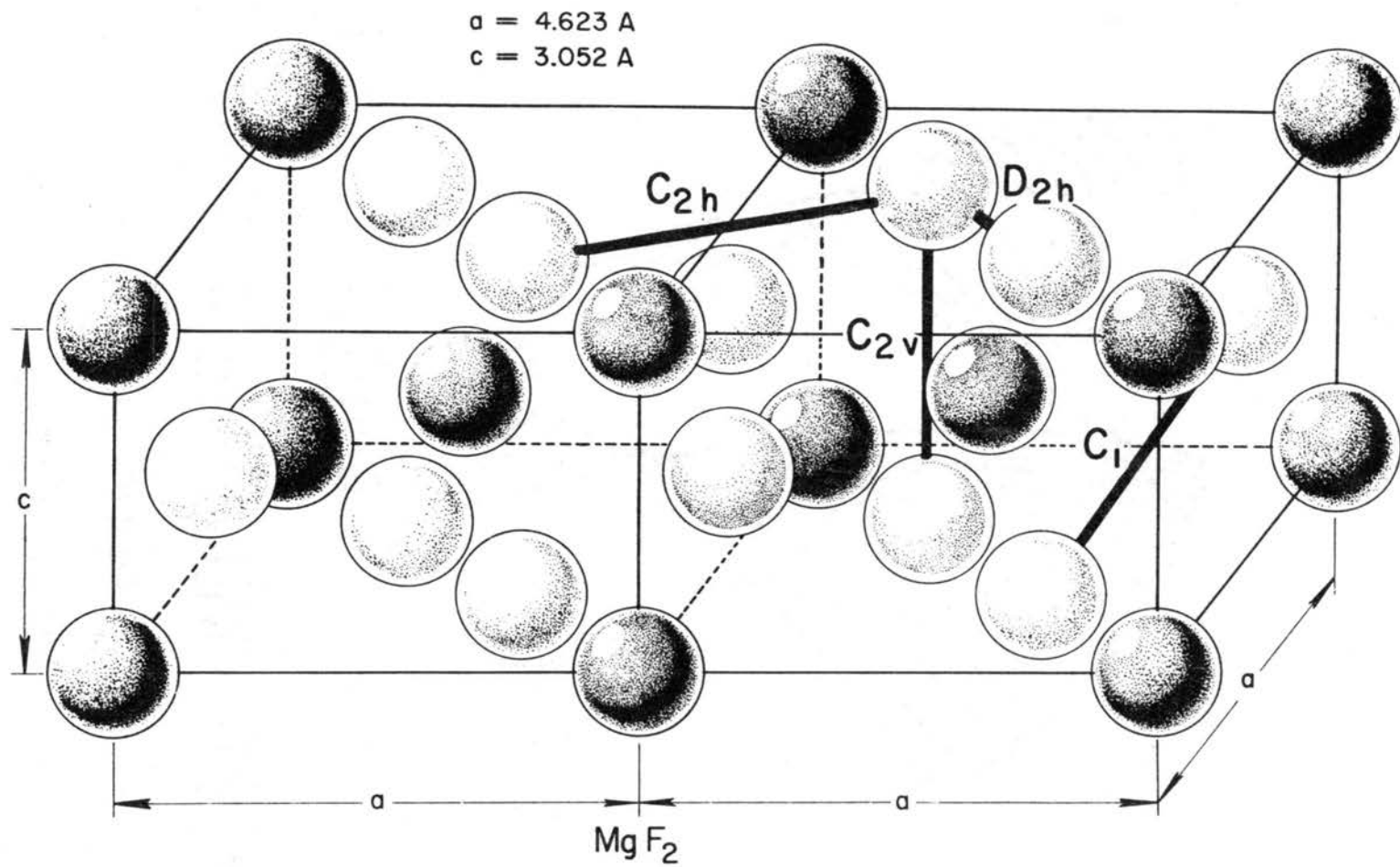
Figure 1.   Two Unit Cells for MgF₂

Another type of M center formed from adjacent anion sites in the top plane of the unit cell has monoclinic C_{2h} symmetry. This type is identified by the label C_{2h} in Figure 1. The longitudinal axis of this type of center lies at an angle of about 11° from the [110] axes. Although there are four equivalent $M(C_{2h})$ centers possible, all four have their unique C_2 axis along the c-axis of the crystal.

The fourth and final type of M center has the triclinic C_1 symmetry and is identified in Figure 1 as C_1. The longitudinal axis of this type of center lies along approximate [011] axes, allowing for sixteen equivalent variations of this type of M center.

Because of these symmetry considerations, it is reasonable to expect polarization studies of the absorption bands of MgF_2 to help distinguish between various types of M_2 centers. The major axes of the $M(C_{2h})$ and $M(D_{2h})$ centers are expected to absorb light polarized such that the electric vector of the incident light is perpendicular to the c-axis of the crystal (E⊥C), while the major dipole of the $M(C_{2v})$ center should absorb light polarized parallel to the c-axis (E∥C). The $M(C_1)$ center is expected to be unpolarized, owing to the sixteen orientations throughout the crystal.

Peak Position of the M Band
Absorptions and Emissions

Several theoretical models have been used to investigate the peak positions of the various M absorption and emission bands. However, each of these models has been oversimplified in order to calculate the transition energies. A model that yields some insight into the problem is that of Hermann (10), who used a hydrogen molecule embedded in a contin-

uous dielectric medium as his model. Even though the model gives only approximate results, a reasonably good physical picture of some of the transition energies can be obtained.

The model arises from the idea that the M center should have the same kind of electronic states as does the H_2 molecule. The H_2 molecule may be thought of as being formed by either bringing together two hydrogen atoms or by splitting a helium atom. The process of bringing together two H atoms until finally a He atom is formed allowing a continuous variation of the electronic states of the H atom into those of a He atom. Thus, the states of the H_2 molecule may be named after the states of either atom. Figure 2 shows the correlation between the molecular orbitals of H and He atoms (11). Each of these orbitals can contain two electrons of opposite spin. The various electronic states of the H_2 molecule are obtained by putting the two electrons in various orbitals.

When both electrons are in the lowest orbital (configuration $(1s\sigma)^2$), this is called the ground state and is denoted as Σ_g. The first excited levels are obtained by putting one of the electrons in a higher orbital. If the electron goes into the $2p\sigma$ orbital, which has configuration ($1s\sigma\ 2p\sigma$), then a Σ_u state is formed. The Σ_u state is also formed when the electron goes into the $2s\sigma$ orbital (configuration ($1s\sigma\ 2s\sigma$)). The third possibility is when the electron goes into the $2p\pi$ orbital (configuration ($1s\sigma\ 2p\pi$)), which creates a π_u state.

The ground state is a singlet state due to the opposite electron spins, but the excited states may be either singlets or triplets. Optical transitions are allowed from the Σ_g ground state ($(1s\sigma)^2$) to the Σ_u ($1s\sigma\ 2p\sigma$) and π_u ($1s\sigma\ 2p\pi$) states, thus giving rise to two absorption bands.
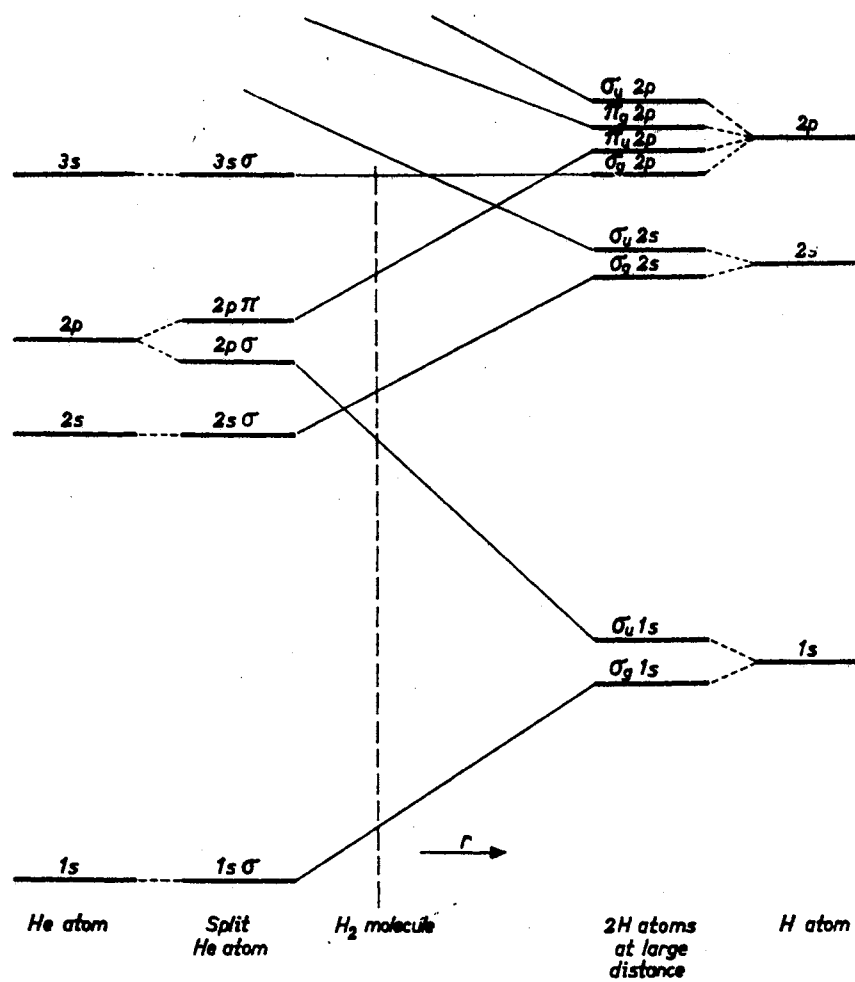
Figure 2. Correlation Diagram of Molecular Orbitals in the He Atom, the H_2 Molecule and the H Atom

The energies of several electronic states of the free hydrogen molecule, as a function of the internuclear distance, are known from experimental data. The energies of a hydrogen molecule in a medium can then be obtained as follows (10,12): The Schrödinger equation for a hydrogen molecule, with electrons of effective mass m*, immersed in a dielectric medium with a dielectric constant ϵ is

$$H\psi \, (\vec{r}_1, \vec{r}_2) \;=\; E\psi \, (\vec{r}_1, \vec{r}_2) \tag{1}$$

where $\vec{r}_1$ and $\vec{r}_2$ are coordinates of the electrons,

$$H \;=\; -\frac{1}{2m^*}(\Delta_1 + \Delta_2) - \frac{1}{\epsilon}\left(\frac{1}{r_{a1}} + \frac{1}{r_{a2}} + \frac{1}{r_{b1}} + \frac{1}{r_{b2}} - \frac{1}{r_{12}} - \frac{1}{r_{ab}}\right) \tag{2}$$

and suffixes 1 and 2 refer to the electrons, a and b to the nuclei. Introducing new coordinates

$$\vec{r}' \;=\; (m^*/\epsilon)\vec{r} \tag{3}$$

yields

$$H'\psi' \, (\vec{r}_{1'}, \vec{r}_{2'}) \;=\; E'\psi' \, (\vec{r}_{1'}, \vec{r}_{2'}) \tag{4}$$

in which

$$E' \;=\; (\epsilon^2/m^*)E \tag{5}$$

The operator H' is identical with the unprimed H except that it is written in terms of the primed variables and does not contain m* and ϵ. Thus the same relation exists between E' and $r_{ab}{'}$ as between E and r_{ab} of the free hydrogen molecule.

The limitations of this model are that in a really continuous

medium, m* should be unity. For the periodic crystal lattice, m* should

be equal to the effective mass of an electron in the nearest allowed

band of electronic states, provided the wave function of the electron

spreads over many lattice points. Since, however, the electron is fair-

ly well localized in the region of the defect, this latter condition is

not fulfilled. For this reason the simple continuum model is not cor-

rect when applied to this defect. The deficiency can be corrected some-

what by means of the semi-continuum model (13,14), where the dielectric

constant is taken to be ε outside the region of greatest electron local-

ization, and unity within the region.

Other models which have been applied to the M-center include the

point-ion approach of Evarestov (15), which produced good agreement with

the actual values of the transition energies of KCl. However, it appears

that the agreement may be fortuitous, since Meyer and Wood (16) have

pointed out that his trial wavefunctions fail to predict the proper F-

center transition energy. Meyer and Wood have themselves calculated the

transition energies of the M center in LiF and LiCl using an extended-

ion approach. The wavefunctions used in this work were those explicitly

found to give the best transition energies for the F center (17). Their

calculated transition energies for the M transitions from the Σ_g state to

Σ_u state were within 10% of the experimentally determined values for both

salts. However, even this scheme appears to have shortcomings in pre-

dicting other transitions energies of the M-center. Further, it appears

to be very difficult to apply to all but the simplest cases, such as the

Lithium halides.

Broadening of the Absorptions and Emission Bands

Experimentally it is observed that absorption and emission peaks are not sharp, but are broadened out in gaussian type bands which center on the peak energies. Perhaps the most common model used to explain this phenomenon is the configuration coordinate model outlined by Fitchen (18), Klick and Schulman (19), and others (20). This model assumes that there is strong coupling to a single lattice coordinate, which is taken to be representative of the displacements of neighboring ions. Usually, it is assumed that these neighboring ions are in a totally symmetric "breathing" mode. In practice, the "single" frequency may turn out to be an average of many phonon mode frequencies, or perhaps a "local" mode, one that is unrelated to the crystal lattice.

A semi-classical approach to the problem seems to be adequate for describing the broad band characteristics of the color centers (20); however, a quantum mechanical treatment sometimes yields other valuable information. One simple way to treat the problem is to assume that electronic states are able to couple in a linear fashion to a single coordinate q of the lattice.

Let us assume that in the M center, there are two nondegenerate electronic states, ψ_g and ψ_e. The Born-Oppenheimer approximation allows electronic motion and nuclear motion to be treated separately, owing to the different effective masses of the two. Thus, the solution of the Schrödinger equation is the product of a nuclear wavefunction and an electronic wavefunction. The nuclear problem is essentially one of solving for the vibronic states for the adiabatic potentials appropriate to the ground and excited states. These potentials are the basis for the schematic configuration coordinate diagram.
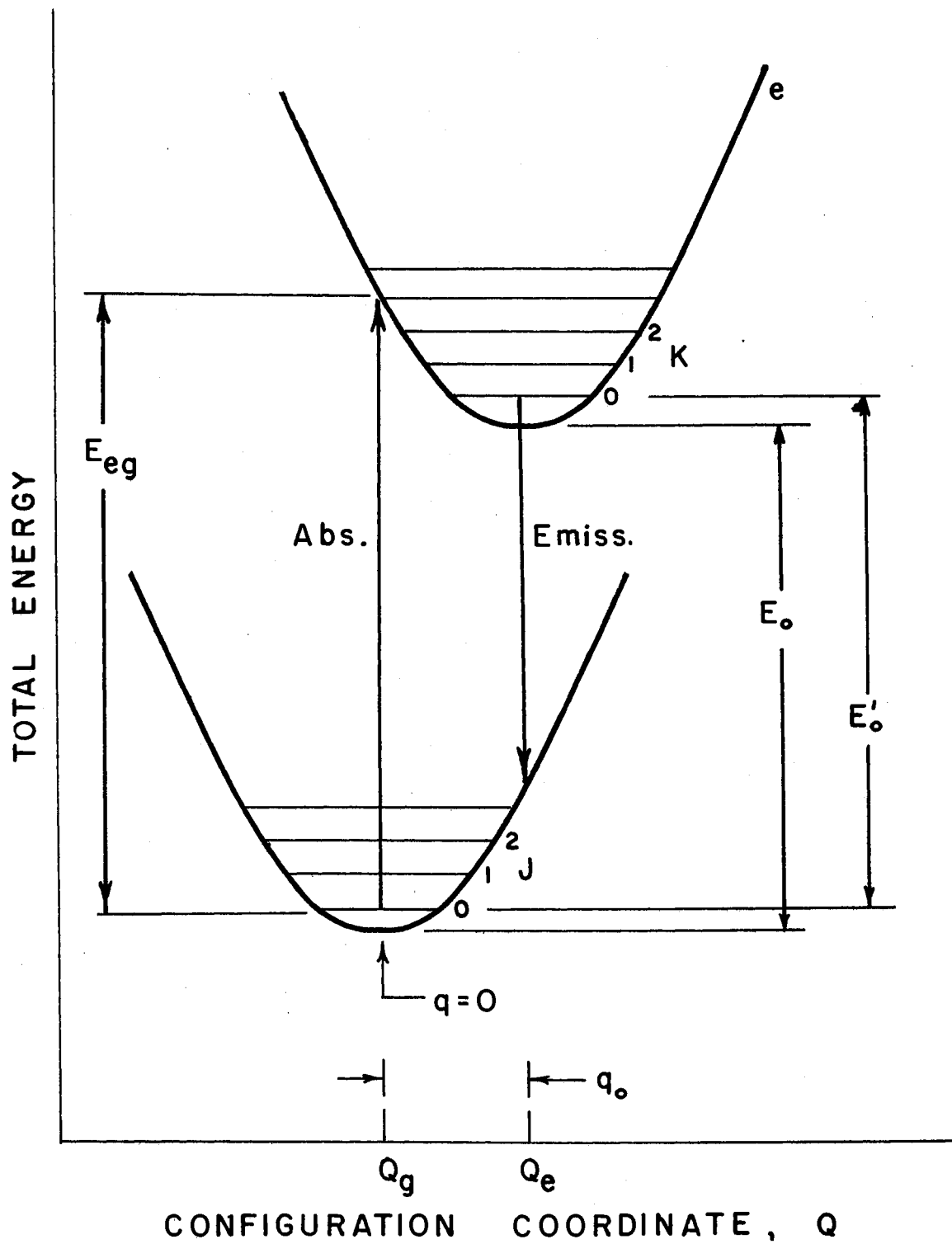
Figure 3. Generalized Configuration Coordinate Diagram

Mathematically, these potentials are described as:

$$E_g = \tfrac{1}{2}M\,\omega^2 q^2 \tag{6}$$

and

$$E_e = \tfrac{1}{2}M\,\omega^2 q^2 + E_{ge} - A\hbar\,\omega(M\omega/\hbar)^{\frac{1}{2}}q \tag{7}$$

where M is the effective mass of the mode, ω is the frequency, and A is a dimensionless constant which acts as a measure of the strength of the linear interaction which acts to displace the equilibrium position of the mode. E_{ge} is the energy separation of the excited state (e) and the ground state (g) potentials, measured at q = 0.

Applying the Born–Oppenheimer approximation at this point means that the width of the absorption or emission lines depend only upon the overlap integral between the ground and excited state wavefunctions. The quantum mechanical solutions, call them $\chi_{gJ}(q)$ and $\chi_{eK}(q)$, are the harmonic oscillator wavefunctions. They have energy eigenvalues:

$$E_{gJ} = (J + \tfrac{1}{2})\,\hbar\omega \tag{8}$$

in the ground state, and

$$E_{eK} = (K + \tfrac{1}{2})\,\hbar\omega + E_{eg} - \frac{1}{2}A^2\hbar\omega \tag{9}$$

in the excited state. The assumption is made here that the mode frequency is the same in both the ground and excited states.

For the coupled defect, the ground and excited state wavefunctions are taken to be product functions, having the form $\psi_g(\vec{r},q)\,\chi_{gJ}(q)$ and $\psi_e(\vec{r},q)\,\chi_{eK}(q)$, where $\vec{r}$ is the electronic coordinate. It is then possi-

ble to calculate the probability for an optical transition at the color center. This probability is proportional to the square of the dipole matrix element $\langle \psi_e \chi_{eK} | \vec{r} | \psi_g \chi_{gJ} \rangle$. (21) Making use of the Condon approximation allows the matrix element to be factored into the product. $\langle \psi_e | \vec{r} | \psi_g \rangle \langle \chi_{eK} | \chi_{gJ} \rangle$, since the electronic dipole moment is assumed to be independent of q, the nuclear coordinate.

Keil (22) has calculated the overlap integral between displaced harmonic oscillator wavefunctions to be:

$$\langle \chi_{eK} | \chi_{gJ} \rangle = \exp\left(-\frac{A^2}{4}\right)\left[\frac{J!}{K!}\right]^{\frac{1}{2}} \left(\frac{A^2}{2}\right)^{\frac{1}{2}(K-J)} L_J^{K-J}\left(\frac{A^2}{2}\right) \tag{10}$$

where $L_J^{K-J}(A^2/2)$ is a Leguerre polynomial. Remembering that A is a dimensionless constant, it seems more convenient to introduce another constant, $S = A^2/2$, which is also dimensionless and will serve as an alternative measure of the coupling strength of the defect. S is commonly called the Huang-Rhys factor (1), and is a measure of the number of phonons involved in the most probable absorption transition.

The normalized transition probability from the ground to the excited state is found from the overlap integral to be

$$W_{KJ} = |\langle \chi_{eK} | \chi_{gJ} \rangle|^2 = e^{-S}\left[\frac{J!}{K!}\right] S^{(K-J)} [L_J^{K-J}(S)]^2 \tag{11}$$

For the case at T = 0 °K, the only ground level state occupied is J = 0. Further, $L_0^K(S) = 1$, and

$$W_{K0} = \frac{S^K}{K!} e^{-S} \tag{12}$$

From this it develops that the absorption spectrum at T = 0 °K consists

of a series of lines such that

$$E_K = (E_{eg} - S\hbar\omega) + K\hbar\omega = E_0 + K\hbar\omega \qquad (13)$$

The series is peaked at n ≅ S. The normalized probability of the zero phonon transition (K = 0) at E_0 is

$$W_{00} = e^{-S} \qquad (14)$$

Thus the probability of seeing the zero phonon transition for a particular color center decreases as a damped exponential as S increases. From a practical viewpoint, a zero phonon transition is likely to be observed only if $S \leq 6$. For values of S greater than six, the area under the zero phonon line is too small relative to the area under the broad band to be observed.

If emission is also possible between the same two states, at low temperatures one would expect the emission spectrum to be a similar series of lines such that

$$E_J = E_0 - J\hbar\omega \qquad (15)$$

These two series would be symmetric about the zero phonon line.

At finite temperatures, levels with J > 0 become thermally populated. To find the line shape for this condition, it is necessary to take a thermal average over all these initial states. If we introduce an index p = K-J that indicates the net number of vibrational quanta excited in the transition, then the absorption spectrum is again a series of lines having energies

$$E_p = E_0 + p\hbar\omega \qquad (16)$$

Keil (22) has calculated the normalized transition probabilities in this
case to be

$$W_p = \exp\left[(p\hbar\omega/2kT) - S\coth(\hbar\omega/2kT)\right]I_p\left[S\coth(\hbar\omega/2kT)\right] \quad (17)$$

where $I_p(z)$ is the Bessel function of the first kind with an imaginary
argument. The widths of these individual transitions with this model
would be limited only by the lifetime of the states.

It is apparent from Figure 3 and Equation (9) that the quantity $S\hbar\omega$
is the energy above the $K = 0$ level at which the absorption maximum
occurs. We may then interpret S to be the number of phonons involved
in the most probable absorption transition. Since the linear coupling
scheme assumes that the mode frequencies in both the ground and excited
states are identical, then the shape of both state functions are identi-
cal, and an identical shift in the emission spectrum is expected. Thus,
the energy difference between the absorption and emission transitions
shown in Figure 3 will be $2S\hbar\omega$. This is referred to as the Stokes shift.

The expression for absorption width at half maximum as a function
of temperature may be found from Equation (17) to be

$$H(T) = H(0)\left[\operatorname{csch}\left(\frac{\hbar\omega}{2kT}\right)\right]^{\frac{1}{2}} \quad (18)$$

The half width at $0^{\circ}K$ is predicted to be

$$H(0) = 2.36\, S^{\frac{1}{2}}\hbar\omega \quad (19)$$

As a comparison, the expression for the absorption halfwidth as a func-
tion of temperature is found semi-classically (1) to be

$$H(T) = H(0)\left[\coth\left(\frac{\hbar\omega}{2kT}\right)\right]^{\frac{1}{2}} \quad (20)$$

which is indistinguishable from (18) in practice.

This leads to a technique for evaluating the Huang-Rhys factor for a broad band transition from experimental measurements. To do so requires an experimental measurement of H(0) and a determination of ω. This latter determination can be accomplished using measurements of H(T) for T > 0. Equation (20) can then be fit to be measured values of H(T), using the value at T = 0 for H(0). A slight variation of this method that produces better results is to plot arc coth $[H^2(T)/H^2(0)]$ vs. 1/T. This plot should yield a straight line through the origin for a proper choice of H(0). Its slope, $\hbar\omega/2k$, may then be used to determine ω, which is the average frequency of the lattice modes involved in the interaction.

CHAPTER III

PROCEDURE

The crystals used in this study were obtained from the Harshaw

Chemical Company and cut such that the c-axis was either parallel to the

face of the crystal $(C_{||})$ or perpendicular to the face $(C_{\perp})$. The samples

were irradiated with either 1.8 MeV electrons from the Oak Ridge National

Laboratory Van de Graaff accelerator, or with 1.5 MeV electrons from the

Oklahoma State University Van de Graaff accelerator.

Optical bleaching was carried out by illuminating the sample with

light from a 100-watt high pressure short arc mercury lamp (PEK 112).

The light was focused with a quartz lens and rendered monochromatic by

passing it through a Spex Industries, 22 cm monochromator. All bleach-

ing was performed at room temperature.

All of the optical absorption measurements were made on a Cary 14

spectrophotometer. The polarized absorption measurements were made using

Polaroid type HNP'B unsupported ultraviolet polarizers in both the sample

and reference beams. The polarization of this system is effective at

wavelengths longer than about 230 nm, and allowed the orientation of the

electric vector of the incident light to be directed along any desired

crystallographic direction of the crystal being studied.

The Cary 14 spectrophotometer records the optical density of the

sample as a function of wavelength. The optical density, O.D. $= \log_{10}$

(I_o/I), where I_o and I are the intensities of the reference and sample

18

beams respectively. The absorption coefficient (α) is a related to the optical density by the prescription:

$$\alpha = 2.303 \ (O.D./t) \ cm^{-1} \tag{21}$$

where t is the sample thickness in cm. Thickness of the samples was measured in several places on the crystal using a micrometer. The average of the measurements was used in calculations.

Luminescence measurements were made using the apparatus shown schematically in Figure 4. The exciting light source was a 75 watt short arc Xenon lamp (PEK X-75) which was passed through a SPEX Industries, Inc., 22 cm Minimate monochromator. The light was then chopped by a Keithley Model 8403-450 light chopper at a frequency of 450 Hz. The chopped light was reflected with a front surface mirror onto the front surface of the sample, which had been rotated slightly off of a 45° angle to minimize the amount of exciting light reflected into the detection system. The luminescence was analyzed with a Jarrell-Ash one-meter Czerny-Turner monochromator having a dispersion of 8.2 $\overset{\circ}{A}$/mm, and detected with an RCA C31034 photomultiplier tube cooled to $-27^{\circ}C$ with a commercial thermoelectric cooler (Products for Research, Inc., Model TE-104). The cooling allowed the photomultiplier tube to be operated at 1800 V DC without excessive dark current. The phototube output was amplified with a Keithley Model 840 lock-in amplifier and the detected luminescence intensity displayed against wavelength on a model 2D-2 X-Y recorder from the F. L. Mosley Company.

Absolute calibration of the exciting light and the detection system were accomplished by S. I. Yun with a quartz iodine standard lamp having calibration traceable to the National Bureau of Standards. The response
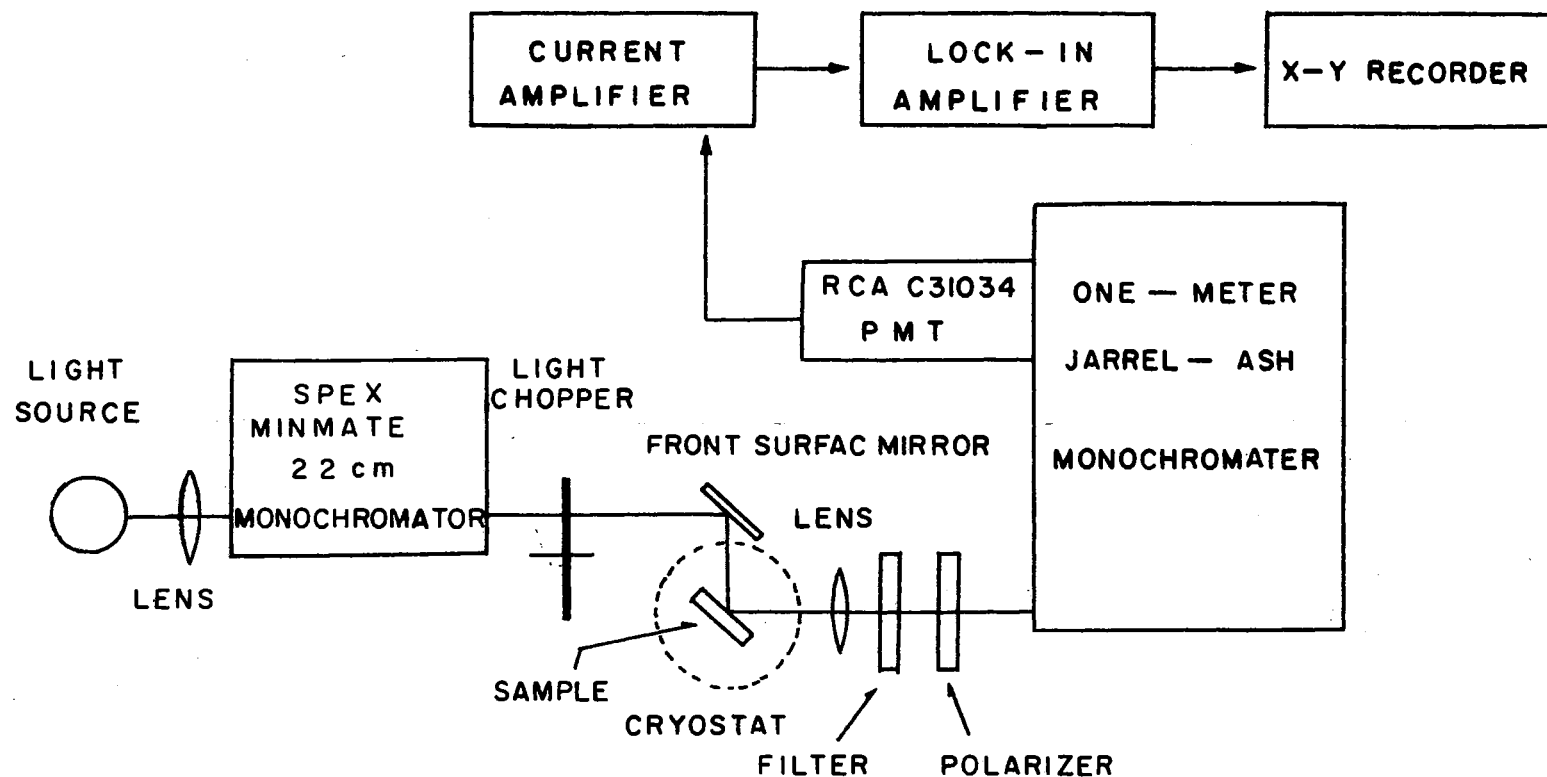
Figure 4. Block Diagram of Luminescence Apparatus

factor of the luminescence detection system as determined from the calibration and the spectral irradiance of the PEK X-75 Xenon short arc lamp are shown in Figures 5 and 6.

The optical excitation spectrum of a luminescence band could be taken with the same apparatus described above, with the exciting light from the SPEX Minimate 22 cm monochromator driven by a synchronous motor drive. The Jarrell Ash one meter monochromator was adjusted to the wavelength of the peak of the luminescence band, and the exciting light was varied from 200 nm up to the wavelength of the emission band by means of the synchronous motor drive. The intensity of the luminescence as a function of the wavelength of the exciting light was displayed on the X-Y recorder. For these studies, care was taken to insure that the natural line widths of the absorption or emission were greater than the instrument resolution. Corning glass filters with optically sharp cut-off's were used to eliminate higher orders of the exciting light from the monochromator output signals.

For all low temperature optical measurements an Air Products and Chemicals, Inc., Model CS-202 Displex helium refrigerator was used. This unit was equipped with a rotatable tail section with quartz windows to allow both absorption and luminescence measurements to made with it. Temperatures between $12^{\circ}K$ and room temperature could be obtained and held accurately for long periods of time by balancing the heat input from an internal resistance heater against the removal of heat by the refrigerator. The sample temperature was measured with a thermocouple consisting of #36 gage gold; 0.7 atomic % iron versus Chromel P wire.
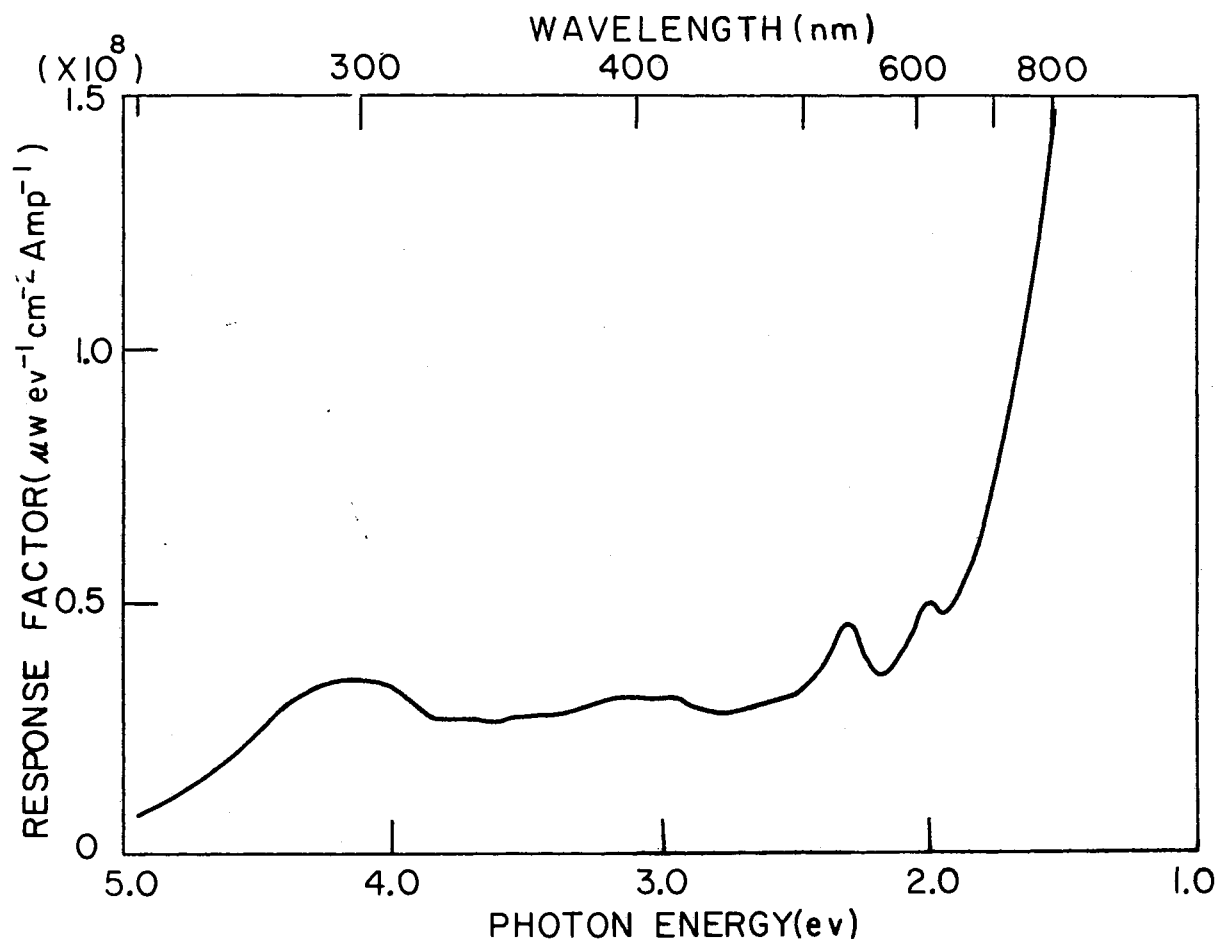
Figure 5.   Response of Luminescence Detection System as a Function
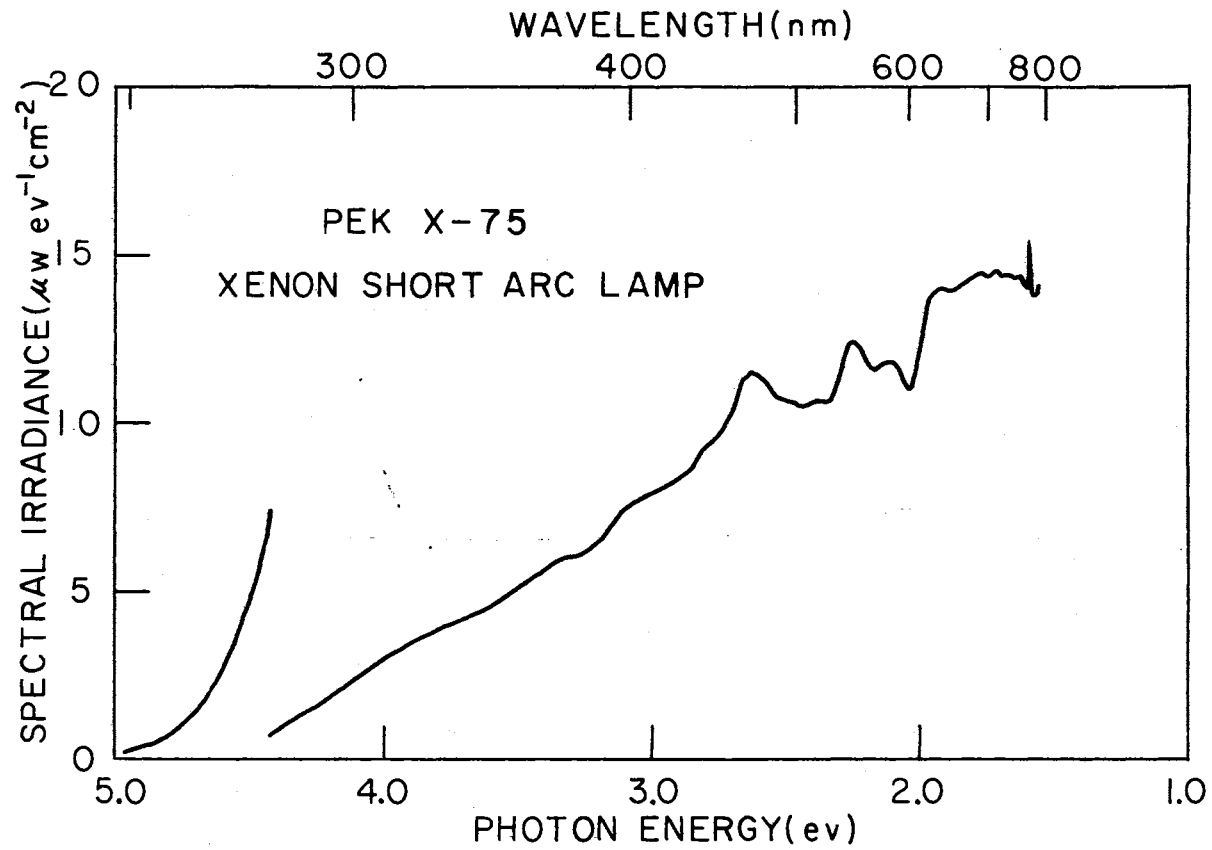of Photon Energy

Figure 6. Spectral Output of PEK X-75 Xenon Short Arc Lamp as a
Function of Photon Energy

CHAPTER IV

PRESENTATION AND DISCUSSION OF RESULTS

Color Center Absorption

The absorption spectra for two samples of MgF_2 which have been electron irradiated at $300^\circ K$ and subsequently optical bleached with 254 nm light are shown in Figure 7. The optical absorption coefficient α, in cm^{-1}, is plotted against the incident photon energy in all three spectra. The sample orientations are noted on the figure, and corrections have been made for the absorption of the polarizers and surface imperfections by use of a double beam instrument and careful subtraction of the absorption of the untreated crystal.

Several of the bands shown have been previously tentatively indentified (24-26). The band at 370 nm has been attributed to the $M(C_{2h})$ center, the one at 400 nm to the $M(C_1)$ center, and the band at 260 nm as due to F centers. The defect responsible for the band at 300 nm has not yet been positively identified, and is of particular importance in this study. Another band, reported by Blunt and Cohen (23) to appear at 320 nm, was observed in this work only by excitation studies. This band has tentatively been identified by these authors to be the $M(D_{2h})$ center absorption.

From the α, π, and σ spectra shown in Figure 7 we can deduce that the absorption bands at 370 nm and 300 nm are electric dipole transitions as one would expect M centers to be. Further, the defects responsible
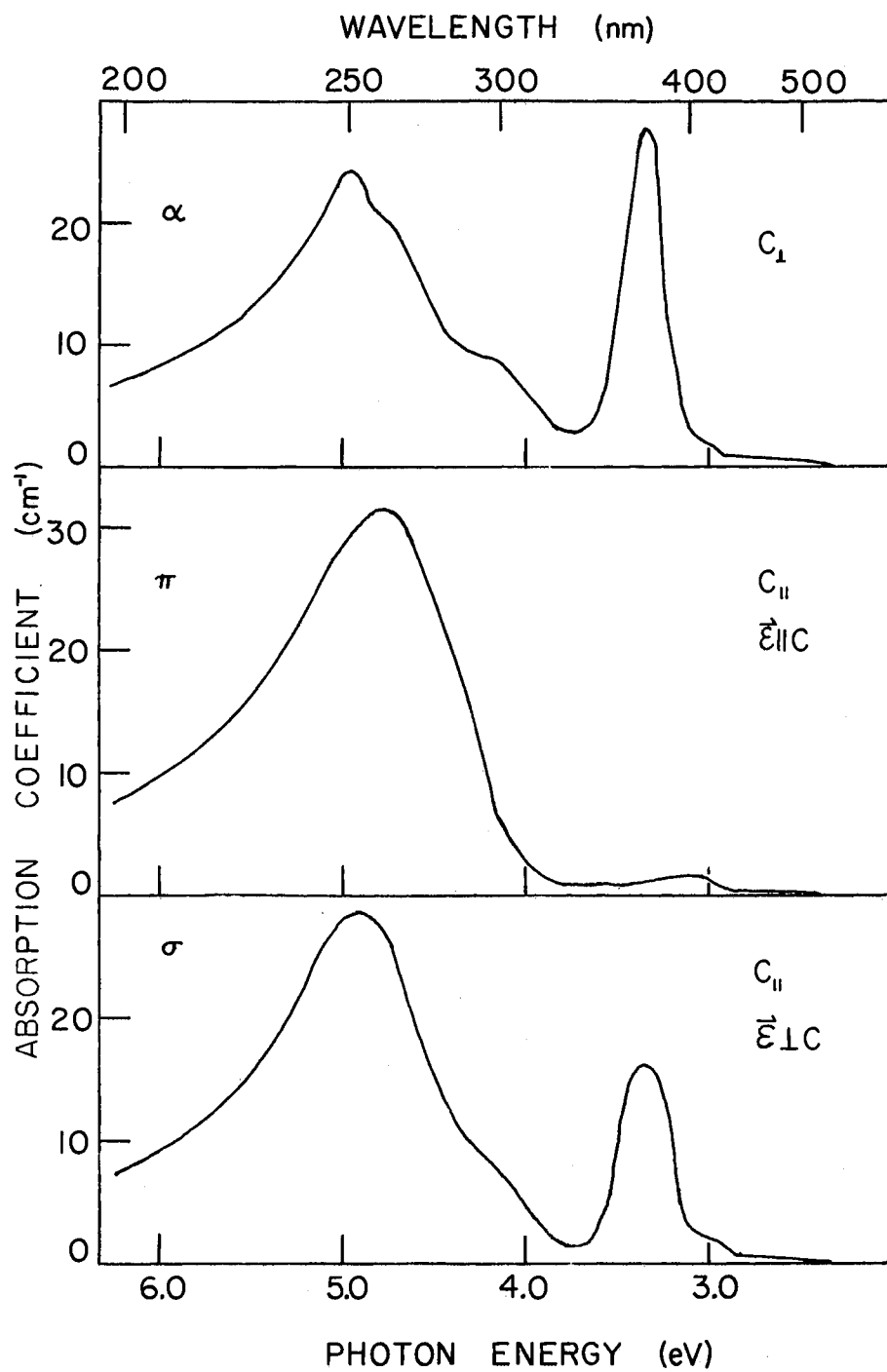
Figure 7. α, π, and σ Absorption Spectra at Room
Temperature for Electron Irradiated
MgF_2 After Optical Bleaching With
254 nm Light

for both bands have orientations that lead to preferential absorption when the electric vector of the incident light is perpendicular to the c-axis of the crystal.

In Figure 8 is plotted the full width at half maximum and the peak position of the 300 nm absorption band as a function of temperature. Figure 9 displays arc coth $(H(T)/H(0))^2$ versus $1/T$ for the same band. From these data it is possible to determine the parameters necessary for the construction of a configuration coordinate diagram for the center. The slope of Figure 9 is a measure of the dominant lattice modes interacting with the defect as discussed in Chapter II. The value determined experimentally, using Equation (20), is $\nu_g = 7.64 \times 10^{12}$ sec^{-1}. The full width at half maximum for $0^\circ K$ was found using computer line-fitting techniques to be 0.276 eV. Using Equation (19) this leads to a value of $S = 13.7$ for the Huang-Rhys factor. This value is too large to allow observation of the zero phonon line, and indeed, no such line is observed.

The growth of absorption coefficient as a function of bleaching time for the absorption bands at 370 nm and 300 nm is illustrated in Figure 10. The former band tends to saturate more quickly and has a higher absorption coefficient than the latter.

A difference curve, which is determined by subtracting the absorption spectrum for a sample before bleaching from the spectrum of that sample after bleach, is displayed in Figure 11. The F band shows a large decrease, whereas the $M(C_1)$ band, and $M(C_{2h})$ band, and the band at 300 nm all show increases in absorption coefficient as a result of the optical bleaching.
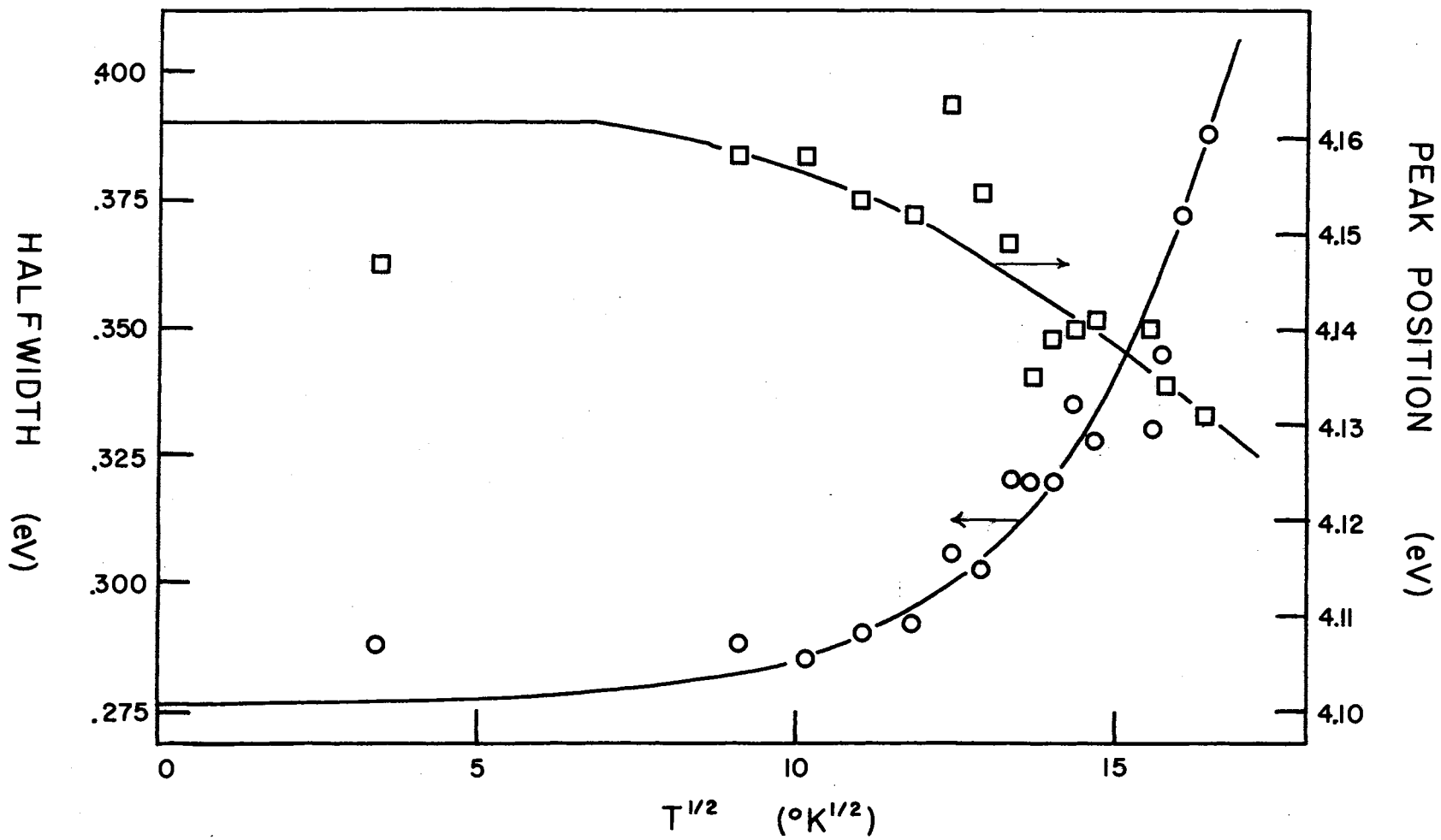
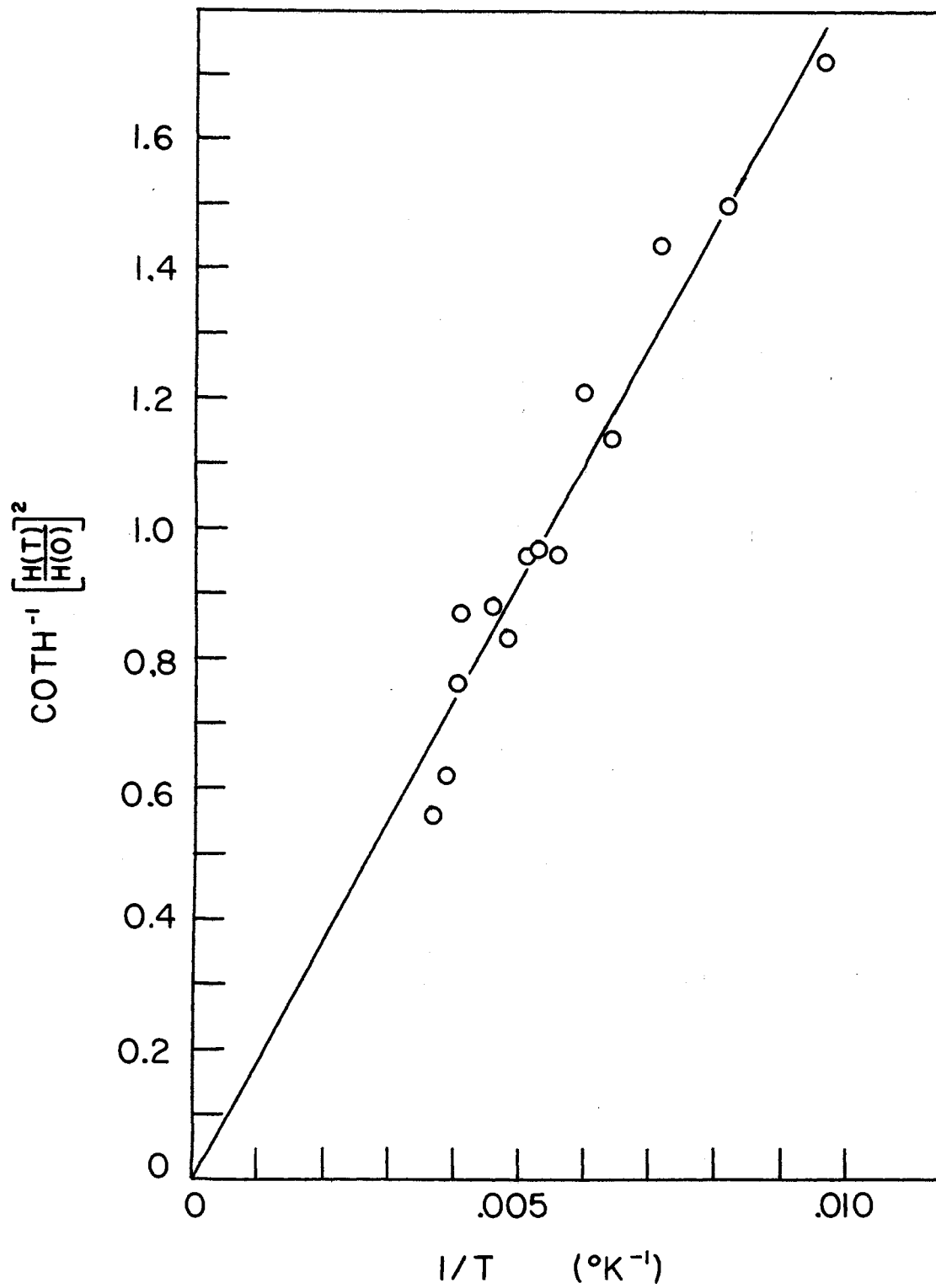Figure 8. Halfwidth and Peak Position of 300 nm Absorption Band as a Function of Temperature

Figure 9. Arc Coth $[H(T)/H(0)]^2$ $\underline{Vs}$. 1/T for 300 nm Absorption Band
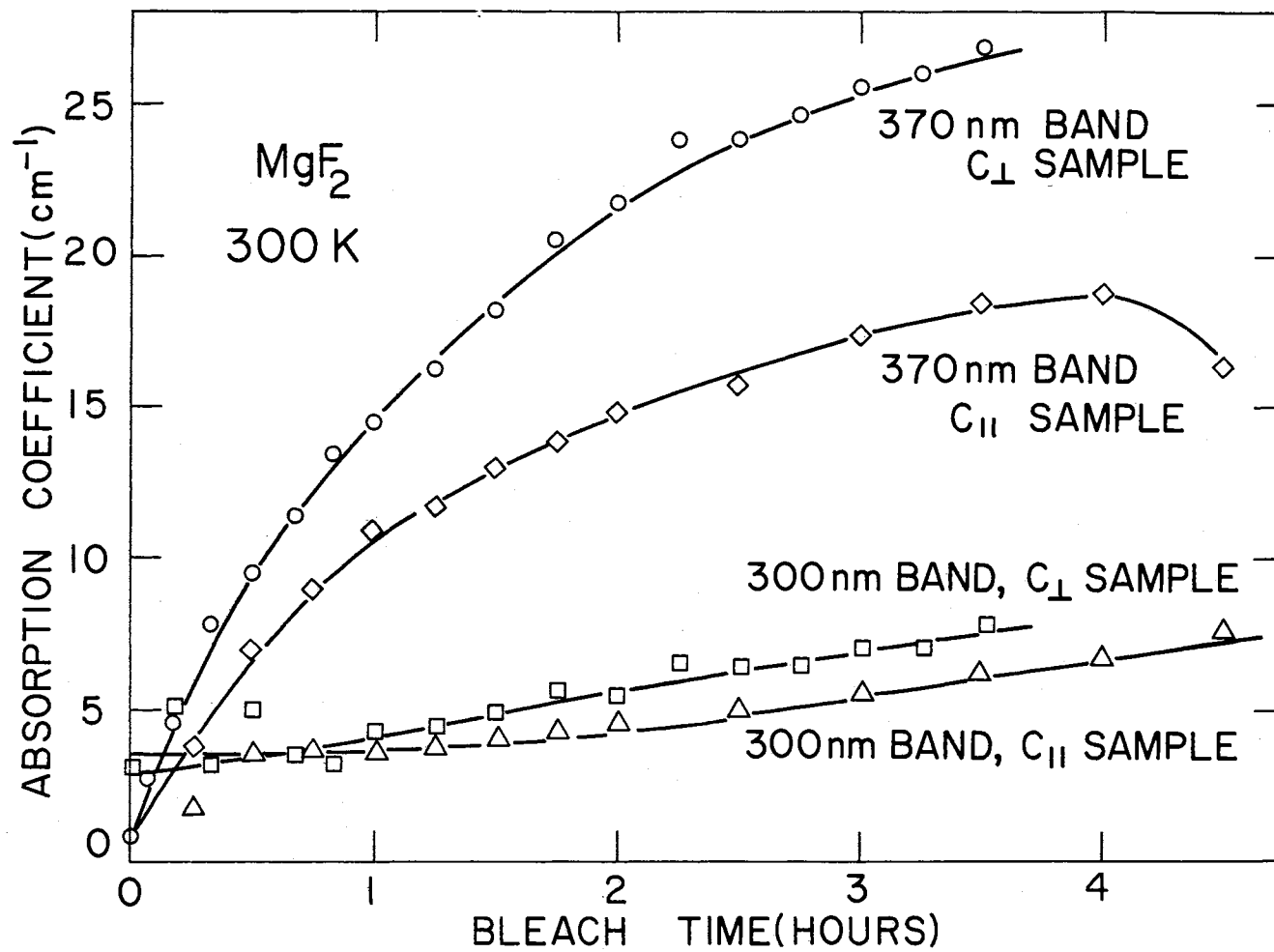
Figure 10. Plot of Absorption Coefficient Vs. Time of Bleach for 300 nm
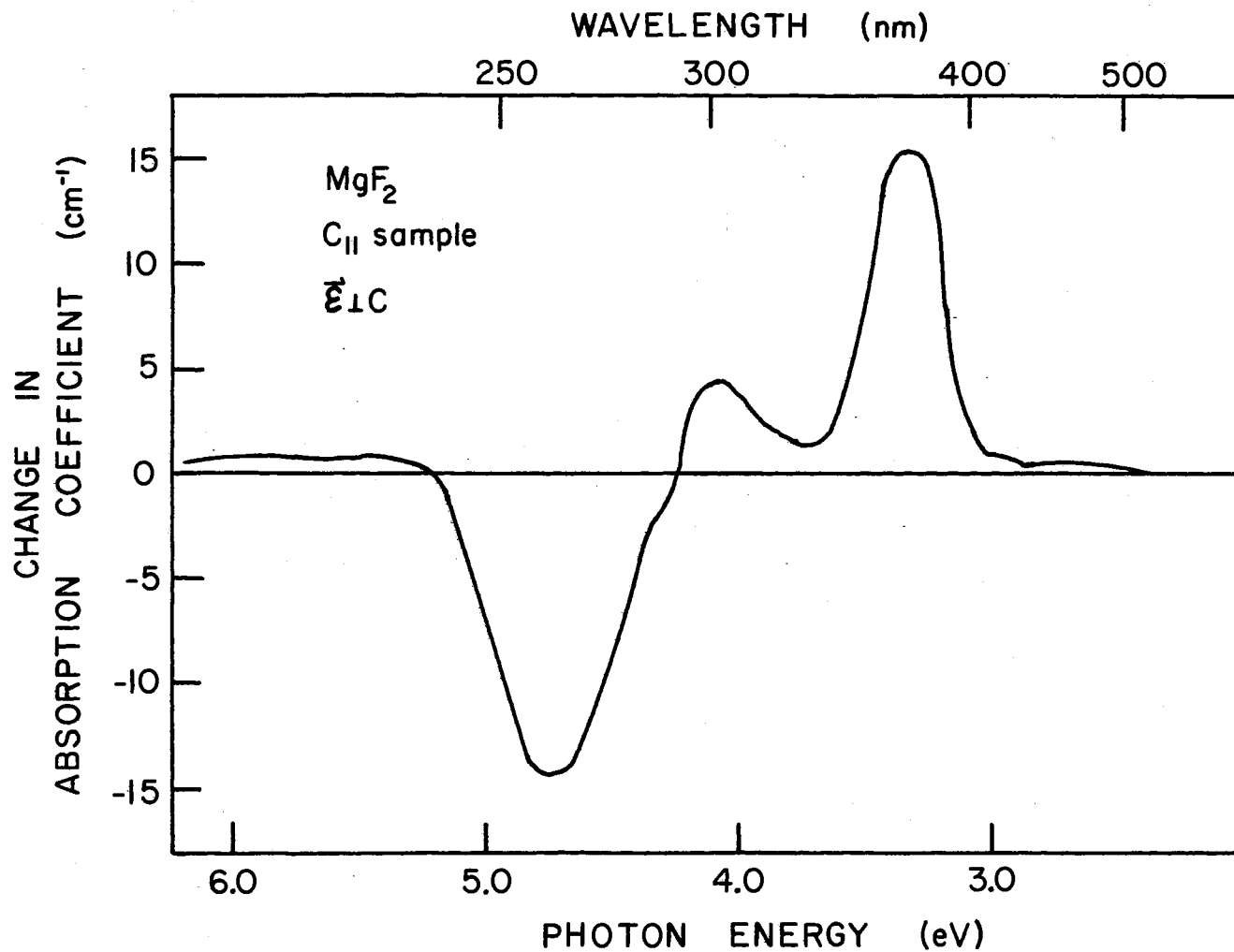and 370 nm Absorption Bands at Room Temperature

Figure 11. Difference Curve for Absorption Spectrum After 4½ Hour
Bleach at Room Temperature

Color Center Emission

Excitation of a color center often results in a luminescent transition back to the ground state. Shown in Figure 12 is the luminescence of a sample of MgF_2 that was electron irradiated and bleached at room temperature for $3\frac{1}{2}$ hours with 254 nm light. The intensity of the luminescence, in arbitrary units, is plotted against incident photon energy. The exciting light is 322 nm, and produced the luminescence shown as the dotted line. At $12^{\circ}K$, the peak position is 460 nm. An excitation spectrum, taken by noting the intensity of luminescence at the peak position as the energy of the exciting light is varied, is shown as the solid line in Figure 12. This spectrum reveals that the maximum luminescence is produced by exciting light of about 322 nm. Figures 13 and 14 are analogous to similar figures for the absorption band, and from them can be determined the parameters required for the configuration coordinate scheme. For the 460 nm emission band it is found that $\nu_e = 6.8 \times 10^{12}$ sec^{-1}, $H(0) = 0.238$ eV, and for the Huang-Rhys factor, $S = 12.9$. The large value of S again precludes observation of the zero phonon transition.

Discussion

It is now possible to use these data to calculate the approximate Stokes shift of the absorption and emission and further analyze the centers to see if the 300 nm absorption is directly responsible for the observed luminescence at 460 nm. Also, it will be possible to determine if there appears to be any strong coupling between the lattice modes and the frequency of nearest neighbor vibrations for the defect.

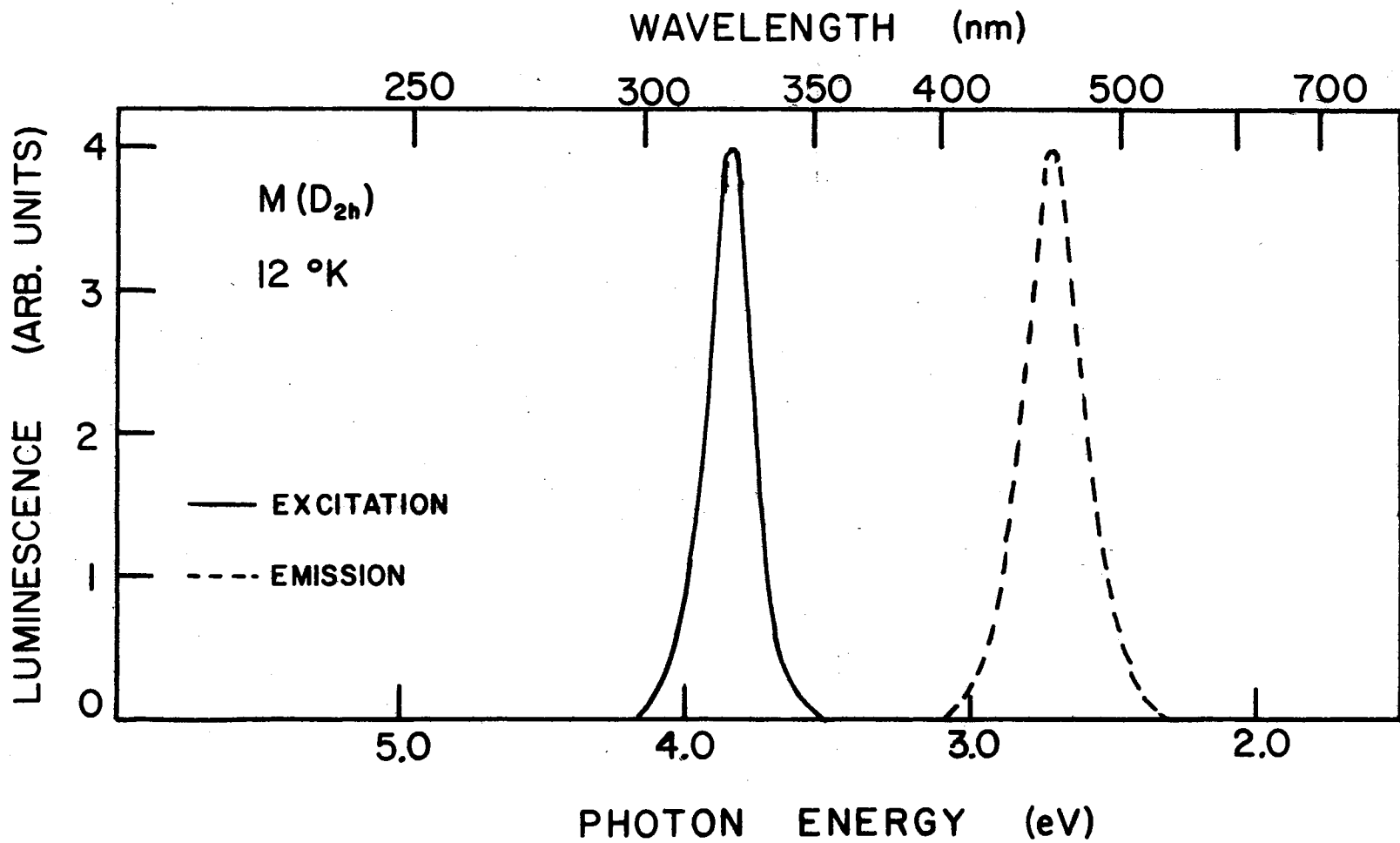The first result is that of the Stokes shift predicted from the ab-

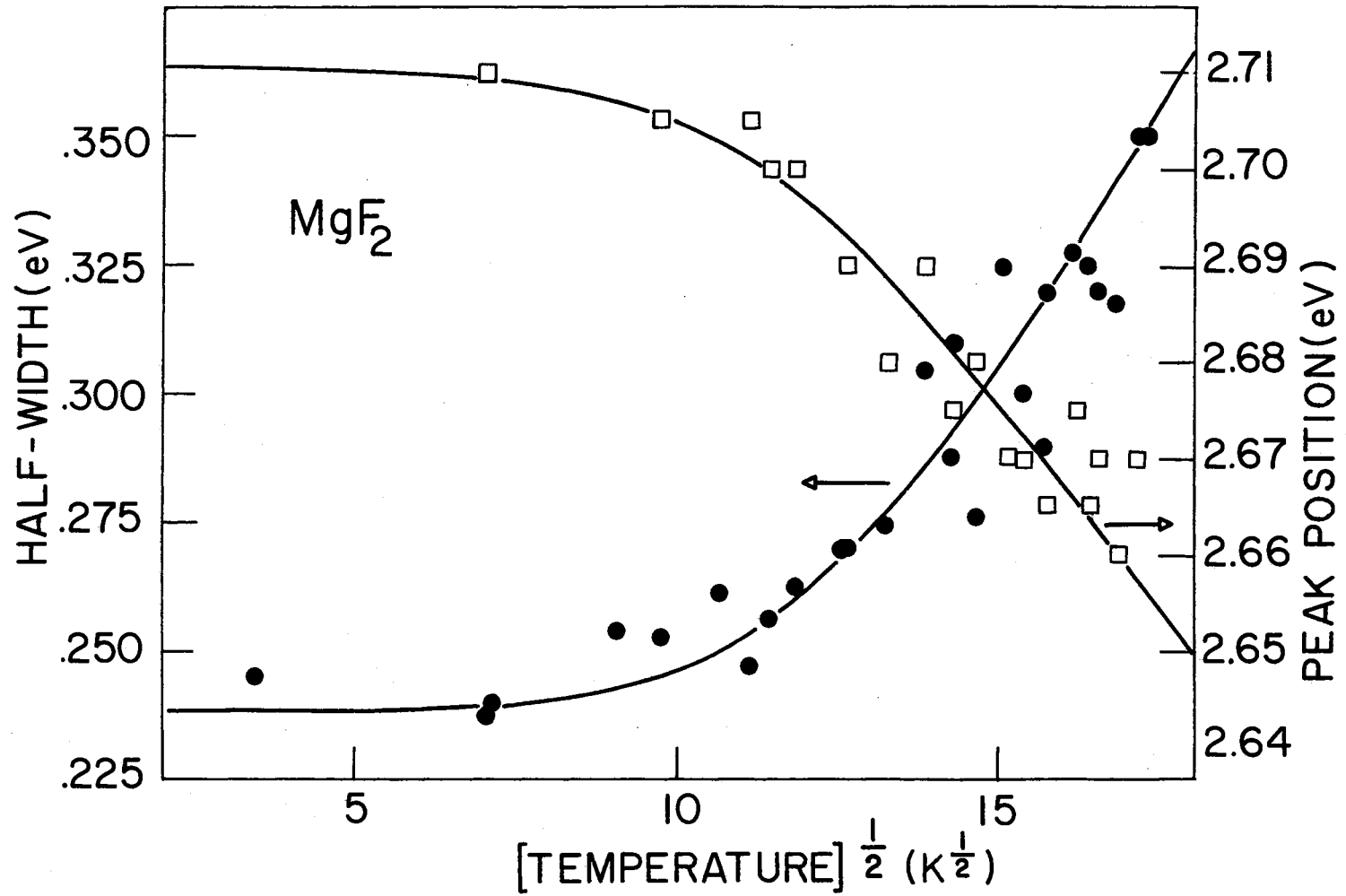Figure 12. Luminescence and Excitation Spectra of 460 nm Emission Band

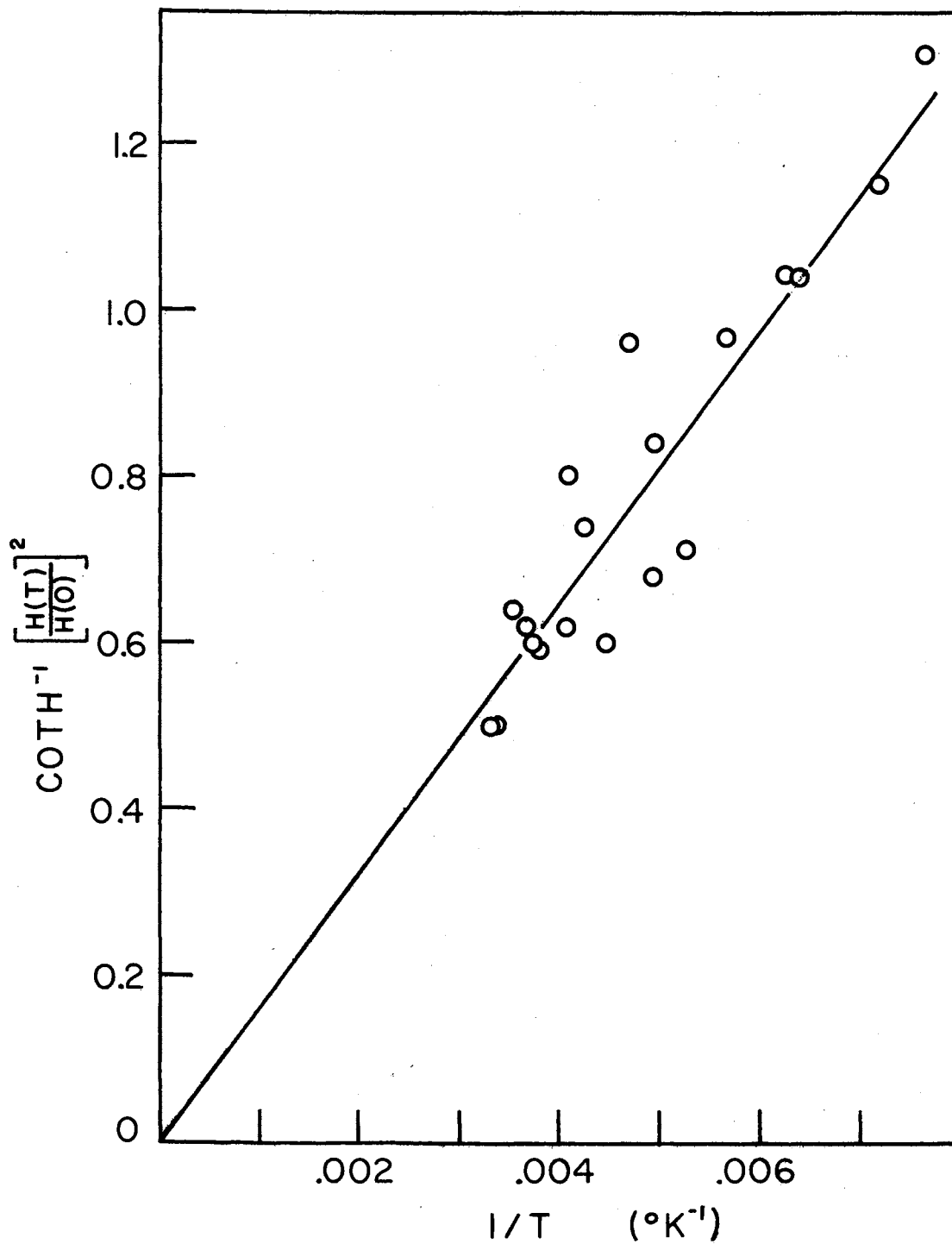Figure 13. Half Width and Peak Position of 460 nm Emission Band as Function of Temperature

Figure 14. Arc Coth $[H(T)/H(0)]^2$ <u>Vs.</u> 1/T for 460 nm Emission Band

sorption data. The absorption peak at 298 nm and the Huang-Rhys factor of 13.7 predict an emission peak for this defect at 372 nm. However, no emission is observed near this wavelength. It is possible that the theory, being only approximate, fails to predict the correct energy for the transition, and it is also possible that this center has a radiationless transition back to the ground state, so that no luminescence is observed.

Using the Stokes shift to predict the absorption peak of the 460 nm emission band yields a value of 364 nm. From the excitation spectrum shown in Figure 12, it is fairly certain that the actual peak of the absorption band responsible for this emission is at 322 nm. The failure of this scheme to accurately predict the absorption band is not totally unexpected, as the error associated with the halfwidth of the excited state is much greater than that of the ground state. However, the excitation spectrum leaves little doubt that the 300 nm band is not responsible for the emission at 460 nm.

It further appears that the 300 nm absorption band is not associated with the 460 nm emission since when a sample was subjected to temperatures above room temperature, a partial annealing of the defects responsible for the 300 nm band occurred. When the sample was rebleached under the same conditions as before the 300 nm band grew back in, but the full width at half maximum of the band was reduced and the peak position at temperatures above $100^{\circ}K$ was shifted significantly. The emission band however appeared to be unaffected, both in half width and peak position. Thus, the absorption and emission bands appear to be due to different defects.

The inability to observe the 320 nm band in the absorption studies,

and to determine the necessary parameters for the configuration coordin-
ate scheme, impaired the study of a single type of defect. If the
assignment by Blunt and Cohen is correct, then the 320 nm absorption,
and thus the 460 nm emission, are due to the $M(D_{2h})$ center. It is not
possible from this investigation to make a tentative assignment other
than what has already been made.

One rather rough way of checking the assignment is by noting the
energies of the ground and excited state vibrational modes, to see if
they correspond to known lattice modes. Although the experimentally de-
rived frequency is an average over all the modes of the crystal, some-
times this approach is helpful. For the absorption band, the energy of
the vibrational mode as determined from Equation (20) is 255 cm^{-1}, and
for the emission it is 227 cm^{-1}. Normal lattice modes that have energies
in a range near these experimentally derived energies are the B_{1u} mode
at 180 cm^{-1}, the E_u mode at 242 cm^{-1}, and the E_g mode at 295 cm^{-1}. (27)

CHAPTER V

SUMMARY AND SUGGESTIONS FOR FURTHER STUDY

Samples of MgF_2 have been irradiated with electrons from a Van de Graaff accelerator and bleached optically with 254 nm light from a mercury source to produce the M bands in the material. These bands were studied by observing their absorption and luminescence characteristics over the range of temperatures from $12^{\circ}K$ to $300^{\circ}K$. From these data the frequency of the dominant interacting phonon mode and the Huang-Rhys factor for the absorption band which peaked near 300 nm and the emission band with a peak near 460 nm were determined. Excitation spectra, determined by measuring the amount of luminescence produced as the exciting light is varied, was used to check the results.

Our findings revealed that the 460 nm emission is produced by a defect which absorbs light of 322 nm. This is not the same as the 300 nm absorption seen on the Cary 14 spectrophotometer, and is quite likely to have considerably less intensity, since it is not observed in the absorption data. Further, no zero phonon lines were found, and evaluation of the calculated Huang-Rhys factors for these broad bands leads to the conclusion that this is reasonable.

Following previous workers (23), tentative assignments have been made for the 320 nm absorption band and the 460 nm emission band, as polarization data indicates these are due to $M(D_{2h})$ centers. No assignment has been attempted for the 300 nm absorption band.

The most obvious suggestion for further study is to grow in the 320 nm absorption band and study it with the same techniques as in this study. From this knowledge the defect could be completely studied from the configuration coordinate scheme.

Another suggestion would be to determine just exactly what defect is responsible for the 300 nm absorption band, and whether or not there is a luminescence associated with the defect.

Studies of these defects in MgF_2 crystals doped with ions from the 3d transition elements, such as Mn, Ni, Co, and Fe, would yield information concerning the M_A type defect. It is possible that impurities in the supposedly pure crystals used in this study are responsible for some of the characteristics observed in this investigation, but since few results are available from doped samples, studies of such doped crystals need to be made to allow for adequate comparison. Also, the perturbing effect of the impurity ion upon the defect may improve certain characteristic such as lifetime so that such a crystal would be better suited for application.

Finally, a search involving electron spin resonance (ESR) techniques would help determine more positively the presence of the M centers under study. Since the M-center is singlet in the ground state, and thus cannot be studied by ESR, the triplet excited state would be the object of such a search. This has been accomplished in Alkali Halide crystals, but whether it is possible in MgF_2 depends on the lifetime of the triplet state. However, the results of such a search could well justify the difficulty involved.

BIBLIOGRAPHY

(1) Markham, J. J., F-Centers in Alkali Halides, (Academic Press, New York, 1966).

(2) Schulman, J. H., and W. D. Compton, Color Centers in Solids, (McMillan, New York, 1962).

(3) Turner, T. J., N. N. Isenhower, and P. K. Tse, Solid State Comm. 7, 1661 (1969).

(4) Van Doorn, C. Z., Rev. Sci. Instr. 32, 755 (1961).

(5) Vehse, W. E., O. E. Facey, and W. A. Sibley, Phys. Stat. Sol. 1, 679 (1970).

(6) Sonder, E. and W. A. Sibley, In Point Defects in Solids, edited by J. H. Crawford and L. M. Slifkin (Plenum, New York, 1972).

(7) Seitz, F., Rev. Mod. Phys. 18, 384 (1946).

(8) Van Doorn, C. Z., and Y. Haven, Philips Res. Repts. 11, 479 (1956).

(9) Compton, W. D. and H. Rabin, Solid State Physics 16, 121 (1964), edited by F. Setiz and D. Turnbull (Academic Press, New York).

(10) Herman, R., M. C. Wallis, and R. F. Wallis, Phys. Rev. 103, 87 (1956).

(11) Herzberg, G., Molecular Spectra and Molecular Structure, Vol. I., (Van Nostrand, New York, 1950).

(12) Gourary, B. S., and F. J. Adrian, Solid State Physics 10, 127 (1960), edited by F. Setiz and D. Turnbull (Academic Press, New York).

(13) Wang, S. and C. Chu, Phys. Rev. 154, 838 (1967).

(14) Wang, S., Progr. Theoret. Phys. (Kyoto) 34, 193 (1965).

(15) Evarestov, R. A., Opt. Spectry (USSR) 16, 198 (1964).

(16) Meyer, A. and R. F. Wood, Phys. Rev. 133, A1436 (1964).

(17) Wood, R. F. and H. W. Joy, Phys. Rev. 136, A451 (1964).

(18) Fitchen, D. B., In *Physics of Color Centers*, edited by W. B. Fowler (Academic Press, New York, 1968).

(19) Klick, C. C. and J. H. Schulman, Solid State Physics $\underline{5}$, (1957), edited by F. Setiz and D. Turnbull (Academic Press, New York).

(20) Fowler, W. B., In *Physics of Color Centers*, edited by W. B. Fowler, (Academic Press, New York, 1968).

(21) Dexter, D. L., Solid State Physics $\underline{6}$, 353 (1958).

(22) Keil, T. H., Phys. Rev. $\underline{140}$, A601 (1965).

(23) Blunt, R. F. and M. I. Cohen, Phys. Rev. $\underline{153}$, 1031 (1967).

(24) Sibley, W. A. and O. E. Facey, Phys. Rev. $\underline{174}$, 1076 (1968).

(25) Facey, O. E. and W. A. Sibley, Phys. Rev. $\underline{186}$, 926 (1969).

(26) Facey, O. E. and W. A. Sibley, Phys. Rev. $\underline{B2}$, 1111 (1970).

(27) Katiyar, R. S. and R. S. Krishnan, Can. J. Phys. $\underline{45}$, 3079 (1967).

|

VITA

Leonard Norman Feuerhelm, Jr.

Candidate for the Degree of

Master of Science

Thesis: OPTICAL ABSORPTION AND EMISSION FROM M-CENTERS IN MgF_2

Major Field: Physics

Biographical:

Personal Data: Born in Eldora, Iowa, July 9, 1949, the son of
Leonard and Daisy Feuerhelm.

Education: Attended primary school in Albion, Iowa; attended sec-
ondary schools in Cedar Rapids, Iowa, and Burlington, Iowa;
graduated from Burlington High School in 1967; received Bache-
lor of Science from Oklahoma State University with a major in
physics in January, 1971; completed requirements for Master of
Science degree in July, 1973.

Experience: Graduate Teaching Assistant in the Physics Department
at Oklahoma State University (1971-1972); 3-M Company Research
Fellow in Physics Department, of Oklahoma State University
(1972-1973).